

PHYS 7221 - The Three-Body Problem

Special Lecture: Wednesday October 11, 2006, Juhan Frank, LSU

1 The Three-Body Problem in Astronomy

The classical Newtonian three-body gravitational problem occurs in Nature exclusively in an astronomical context and was the subject of many investigations by the best minds of the 18th and 19th centuries. Interest in this problem has undergone a revival in recent decades when it was realized that the evolution and ultimate fate of star clusters and the nuclei of active galaxies depends crucially on the interactions between stellar and black hole binaries and single stars. The general three-body problem remains unsolved today but important advances and insights have been enabled by the advent of modern computational hardware and methods.

The long-term stability of the orbits of the Earth and the Moon was one of the early concerns when the age of the Earth was not well-known. Newton solved the two-body problem for the orbit of the Moon around the Earth and considered the effects of the Sun on this motion. This is perhaps the earliest appearance of the three-body problem. The first and simplest periodic exact solution to the three-body problem is the motion on collinear ellipses found by Euler (1767). Also Euler (1772) studied the motion of the Moon assuming that the Earth and the Sun orbited each other on circular orbits and that the Moon was massless. This approach is now known as the restricted three-body problem. At about the same time Lagrange (1772) discovered the equilateral triangle solution described in Goldstein (2002) and Hestenes (1999). The collinear and equilateral triangle solutions are the only explicit solutions known for arbitrary masses and a handful of solutions for special cases are also known (Montgomery 2001).

The basis for the modern theory of the restricted three-body problem was developed by Jacobi (1836), Delaunay (1860), and Hill (1878). The classical period ends with the powerful methods of surfaces of section, phase space and deterministic chaos developed by Poincaré who was awarded in 1889 the prize established by Sweden's King Oscar II for the first person to solve the n -body problem. Although, strictly speaking, Poincaré did not solve the general 3-body problem, let alone the n -body problem, his insights influenced much of the work that followed.

I will review some of the known exact solutions valid for special cases, sketch out a few aspects of the restricted three-body problem and conclude by discussing some numerical results and astrophysical applications.

2 The General Three-Body Problem

Just as in the two-body problem it is most convenient to work in the center-of-mass (CM) system with \mathbf{x}_i denoting the position of mass m_i . The Newtonian equations of motion in this system are of the form

$$\ddot{\mathbf{x}}_i = -Gm_j \frac{\mathbf{x}_i - \mathbf{x}_j}{|\mathbf{x}_i - \mathbf{x}_j|^3} - Gm_k \frac{\mathbf{x}_i - \mathbf{x}_k}{|\mathbf{x}_i - \mathbf{x}_k|^3} \quad (1)$$

where i, j, k stand for 1, 2, 3 and the two ordered permutations of these indexes. These three second-order vector differential equations are equivalent to 18 first order scalar differential equations. The CM condition and its first derivative

$$\sum_{i=1}^{i=3} m_i \mathbf{x}_i = 0 \quad (2)$$

$$\sum_{i=1}^{i=3} m_i \dot{\mathbf{x}}_i = 0 \quad (3)$$

are 6 constraints that reduce the order of the system to 12. In the absence of external forces and torques, the energy and angular momentum are conserved quantities or integrals of the motion. These further reduce the order of the system to $12 - 4 = 8$. As in the two-body problem, one could eliminate the time and reduce the order by one, and using an analog procedure to fixing the line of nodes, reduce it again to 6. Even if the motion was restricted to a plane fixed in space, the order is reduced to 4 which is still unsolvable in general.

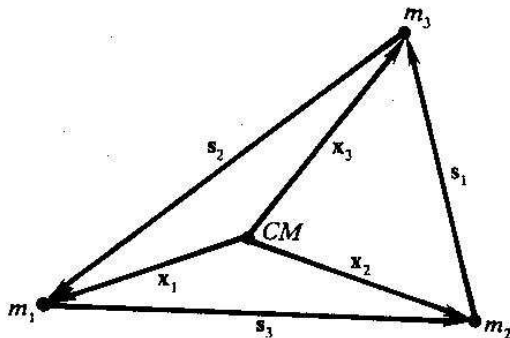


Figure 1: Position vectors in the CM system and relative position vectors for the three-body problem (Hestenes 1987).

In 1973 Broucke & Lass realized that the equations of motion could be written in a more symmetrical form by using the relative position vectors $\mathbf{s}_i = \mathbf{x}_j - \mathbf{x}_k$, labeled in such a way that the \mathbf{s}_i is the side opposite to the vertex of the triangle containing the mass m_i (see Fig. 1) and that

$$\mathbf{s}_1 + \mathbf{s}_2 + \mathbf{s}_3 = 0. \quad (4)$$

In terms of these relative position vectors, the equations of motion (1) adopt the symmetrical form

$$\ddot{\mathbf{s}}_i = -GM \frac{\mathbf{s}_i}{s_i^3} + m_i \mathbf{G}, \quad (5)$$

where $M = m_1 + m_2 + m_3$ is the total mass and the vector \mathbf{G} is given by

$$\mathbf{G} = \sum_{i=1}^{i=3} \frac{\mathbf{s}_i}{s_i^3} \quad (6)$$

Note that the first term on the r.h.s of (5) is identical to what one gets in the standard treatment of the two-body Kepler problem, which admits conic sections as orbital solutions. It is the second term that is responsible for the difficulty in this problem since it couples the equations for the \mathbf{s}_i .

3 Euler's Solution

If all particles are collinear, all the vectors \mathbf{s}_i , \mathbf{x}_i and \mathbf{G} are proportional to one another. Without loss of generality let's suppose that m_2 lies in between the other two masses. Then \mathbf{s}_3 points from

m_1 to m_2 , \mathbf{s}_1 points in the same direction and sense as \mathbf{s}_3 from m_2 to m_3 , and \mathbf{s}_2 points back from m_3 to m_1 . Therefore, we can write

$$\mathbf{s}_1 = \lambda \mathbf{s}_3, \quad \mathbf{s}_2 = -(1 + \lambda) \mathbf{s}_3, \quad (7)$$

where λ is a positive scalar. Expressing everything in the equations of motion in terms of \mathbf{s}_3 and λ , one obtains after some algebra (see Hestenes 1987 for details) a fifth degree polynomial in λ with one single positive real root which is a function of the three masses; and, \mathbf{s}_3 obeys a two-body equation of the form

$$\ddot{\mathbf{s}}_3 = -\frac{m_2 + m_3(1 + \lambda)^{-2}}{m_2 + m_3(1 + \lambda)} \frac{GM\mathbf{s}_3}{s_3^3}. \quad (8)$$

Thus the particles move along confocal ellipses of the same eccentricity (i.e. similar ellipses) and the same orbital period around the common center of mass, always lined up and separated by distances obeying eq. (7). This describes one family of solutions. The other two families can be found by putting one of the other particles in the middle. On a sober note, these collinear solutions are not realized in nature because they are unstable to small perturbations.

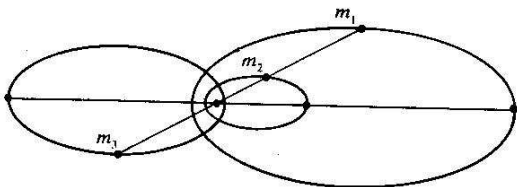


Figure 2: Euler's collinear solution for masses in the ratio $m_1 : m_2 : m_3 = 1 : 2 : 3$ (Hestenes 1987).

4 Lagrange's Solution

This case is realized when $\mathbf{G} = 0$ and the equations for the \mathbf{s}_i decouple. The three decoupled equations have the two-body form whose solutions are ellipses for bound cases. The condition for $\mathbf{G} = 0$ is that $s_1 = s_2 = s_3$, in other words the particles sit at the vertexes of an equilateral triangle at all times, even as this triangle changes size and rotates (see Fig. 3). Each particle follows an ellipse of the same eccentricity but oriented at different angles, with the common center of mass at the focal point of all three orbits. The motion is periodic with the same period for all three particles. The Lagrange solution is stable only if one of the three masses is much greater than the other two. Montgomery (2001) describes several other solutions that exist when all the particles have the same mass, e.g. a figure-eight solution for 3 particles, which is stable, and even more complicated solutions with up to eleven (!) particles. Although these exact solutions are fun, they are of very little practical importance since they require very special initial conditions to be realized.

5 The Pythagorean Problem

Burrau (1913) considered a well defined but arbitrarily selected initial configuration of three bodies of masses 3, 4 and 5 placed at the corners of a Pythagorean triangle facing sides of length proportional

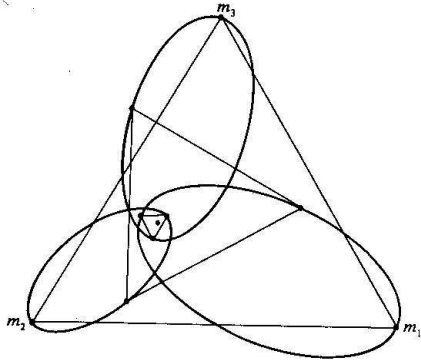


Figure 3: Lagrange's equilateral triangle solution for masses in the ratio $m_1 : m_2 : m_3 = 1 : 2 : 3$ (Hestenes 1987).

to each mass. The initial configuration is shown on Fig. 4. The masses are at rest initially and begin to move due their mutual attraction. After a very complex interaction, the two heavier masses bind in a stable binary while the light object escapes, and all particles recede without limit from the common center of mass. Fig. 5 shows the time-development of the orbital paths of the three

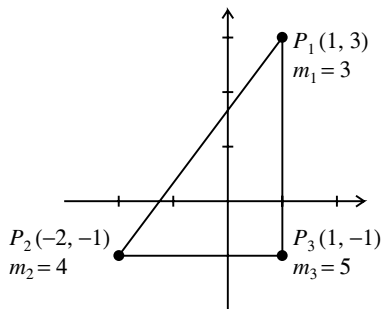


Figure 4: Initial configuration for Burrau's pythagorean problem shown in the CM reference frame. The masses are in the ratios $m_1 : m_2 : m_3 = 3 : 4 : 5$ and are released from rest (Valtonen & Karttunen 2006).

particles. This behavior turns out to be quite common when three particles of roughly comparable masses are allowed to interact gravitationally with randomly selected initial conditions. Modern computer experiments have explored the outcomes of hundreds of thousands of initial configurations and have allowed the development of a statistical understanding of the interactions between three particles, of a binary with a third object and of binaries with binaries.

6 The Restricted Three-Body Problem: Roche's Potential

We illustrate the standard techniques involved in the restricted three-body problem by considering the motion of gas, or alternatively non-interacting particles, in and around an interacting binary with a circular orbit (adapted from Frank, King & Raine 2002). Non-interacting particles feel the

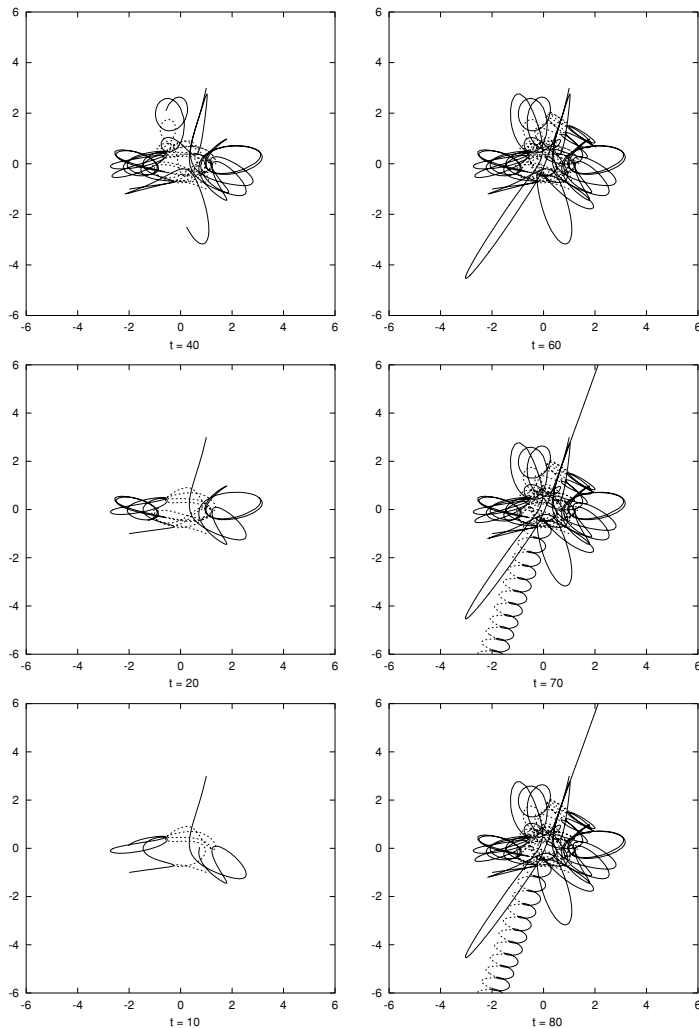


Figure 5: Trajectories for Burrau’s pythagorean problem shown in the CM reference frame. The last two panels are identical since both the binary and the light particle have left the frame (Valtonen & Karttunen 2006).

“external” gravity of the stars but do not interact with each other. The motion of gas is subject to pressure gradient forces in addition to gravity of the stars. The mass of the particles or fluid elements is almost always negligible compared to the masses of the binary components and thus induces negligible accelerations on the stars. Under these conditions the binary components orbit the common center of mass on circular orbits of constant radius and will be at rest in a suitably chosen corotating frame.

Any gas flow between the two stars is governed by the Euler equation:

$$\frac{d\mathbf{v}}{dt} = \frac{\partial\mathbf{v}}{\partial t} + (\mathbf{v} \cdot \nabla)\mathbf{v} = -\nabla\Phi - \frac{1}{\rho}\nabla P, \quad (9)$$

where Φ is the gravitational potential of the stars. For non-interacting particles we drop the pressure gradient and *advective* terms and integrate directly $\dot{\mathbf{v}}$ following the particle's motion.

It is convenient to write this in a frame of reference rotating with the binary system, with angular velocity ω relative to an inertial frame, since in the rotating frame the two stars are fixed. This introduces extra terms in the Euler equation to take account of centrifugal and Coriolis forces. With the assumptions made for the Roche problem, the Euler equation takes the form

$$\frac{\partial \mathbf{v}}{\partial t} + (\mathbf{v} \cdot \nabla) \mathbf{v} = -\nabla \Phi_{\text{R}} - 2\omega \wedge \mathbf{v} - \frac{1}{\rho} \nabla P, \quad (10)$$

with the angular velocity of the binary, ω , given in terms of a unit vector, \mathbf{e} , normal to the orbital plane by

$$\omega = \left[\frac{GM}{a^3} \right]^{1/2} \mathbf{e}.$$

The term $-2\omega \wedge \mathbf{v}$ is the Coriolis force per unit mass; $-\nabla \Phi_{\text{R}}$ includes the effects of both gravitation and centrifugal force. Φ_{R} is known as the Roche potential (Fig. 6) and is given by

$$\Phi_{\text{R}}(\mathbf{r}) = -\frac{GM_1}{|\mathbf{r} - \mathbf{r}_1|} - \frac{GM_2}{|\mathbf{r} - \mathbf{r}_2|} - \frac{1}{2}(\omega \wedge \mathbf{r})^2 \quad (11)$$

where \mathbf{r}_1 , \mathbf{r}_2 are the position vectors of the centres of the two stars. We gain considerable insight into accretion problems by plotting the equipotential surfaces of Φ_{R} and, in particular, their sections in the orbital plane (Fig. 7). When doing this, we must be careful to remember that some of the forces, in particular the Coriolis forces, acting on the accreting gas are not represented by Φ_{R} .

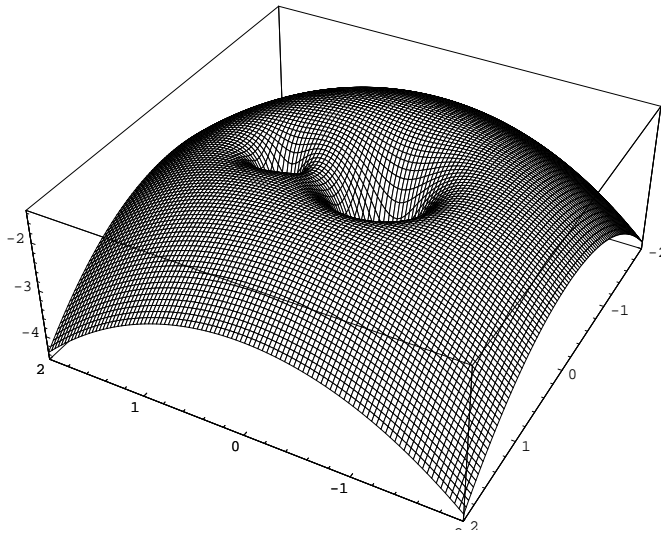


Figure 6: A surface representing the Roche potential for a binary system with mass ratio $q = M_2/M_1 = 0.25$ (the same as in Fig. 7). The larger pit is around the more massive star. The downward curvature near the edges is due to the ‘centrifugal’ term; a test particle attempting to corotate with the binary at these distances experiences a net outward force.

The shape of the equipotentials is governed entirely by the mass ratio q , while the overall scale is given by the binary separation a . Figure 7 is drawn for the case $q = 0.25$, but its qualitative features apply for any mass ratio. Matter orbiting at large distances ($r \gg a$) from the system sees it as a point mass concentrated at the centre of mass (CM). Thus, the equipotentials at large distances are just those of a point mass viewed in a rotating frame. Similarly, there are circular equipotential sections around the centres of each of the two stars ($\mathbf{r}_1, \mathbf{r}_2$); the motion of matter here is dominated by the gravitational pull of the nearer star. Hence, the potential Φ_R has two deep valleys or pits centred on $\mathbf{r}_1, \mathbf{r}_2$. The most interesting and important feature of Fig. 7 is the figure-of-eight area (the heavy line), which shows how these two valleys are connected. In three dimensions, this ‘critical

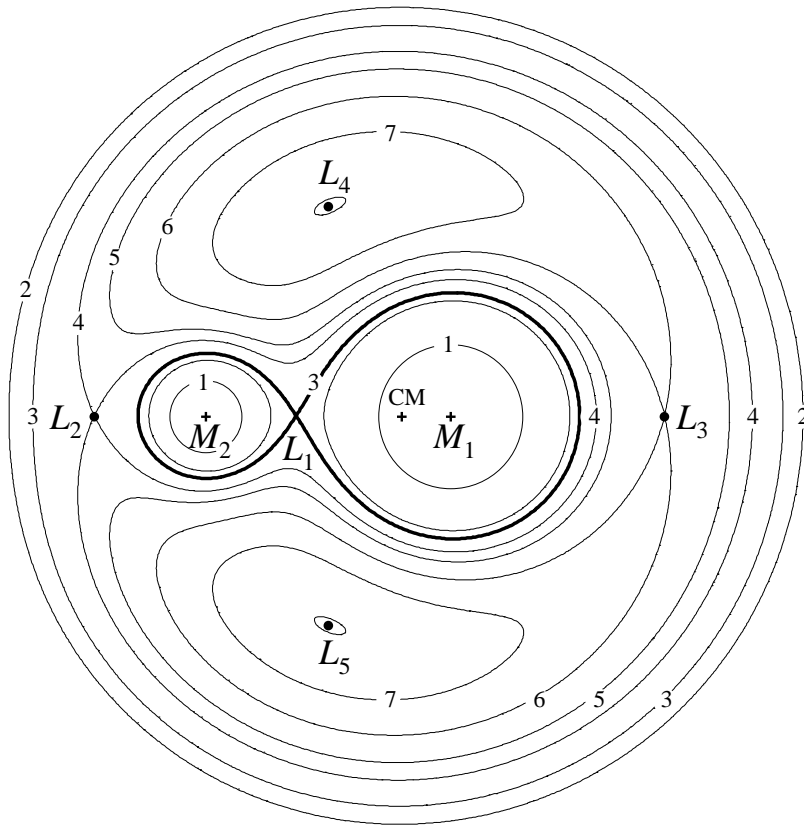


Figure 7: Sections in the orbital plane of the Roche equipotentials $\Phi_R = \text{constant}$, for a binary system with mass ratio $q = M_2/M_1 = 0.25$. Shown are the center of mass (CM) and Lagrange points L_1 – L_5 . The equipotentials are labeled 1–7 in order of *increasing* Φ_R . Thus the saddle point L_1 (the inner Lagrange point) forms a ‘pass’ between the two ‘Roche lobes’, the two parts of the figure-of-eight equipotential 3. The Roche lobes are roughly surfaces of revolution about the line of centers M_1 – M_2 . L_4 and L_5 (the ‘Trojan asteroid’ points) are local maxima of Φ_R but Coriolis forces stabilize synchronous orbits of test bodies at these points.

surface' has a dumbbell shape; the part surrounding each star is known as its *Roche lobe*. The lobes join at the *inner Lagrange point* L_1 , which is a saddle point of Φ_R ; to continue the analogy, L_1 is like a high mountain pass between two valleys. This means that material inside one of the lobes in the vicinity of L_1 finds it much easier to pass through L_1 into the other lobe than to escape the critical surface altogether.

The two off-axis Lagrange points L_4 and L_5 are local maxima of the effective potential, and are unstable at first sight. However, Coriolis forces act to confine the orbits of particles released in the vicinity of these points. A more careful treatment shows that orbits around L_4 and L_5 are stable provided that $(M_1 - M_2)/M > (23/27)^{1/2}$ (Hestenes 1987) or $q < 0.04$. It also turns out that the collinear saddle points L_1 , L_2 and L_3 are capable of supporting stable quasi-periodic orbits known as "halo" orbits. In fact, several of the best known past and future NASA missions were or are planned to go on libration orbits around L_1 (SOHO, LISA) and L_2 (WMAP, NGST).

7 Annotated References

Diacu, F. & Holmes, P., 1996, *Celestial Encounters: The Origins of Chaos and Stability*, Princeton University Press. A Very readable and non-mathematical historical account of the development of the n -body problem, nonlinear dynamics, chaos and stability, including the more recent developments due to Arnold, Kolmogorov, Liapunov, and Moser.

Frank, J., King, A.R. & Raine, D.J., 2002, *Accretion Power in Astrophysics*, Cambridge University Press. An introductory graduate-level book on accretion in binaries and active galactic nuclei. The restricted three-body problem forms the basis for the study of accretion flows in interacting binary stars.

Goldstein, H., Poole, C.P. & Safko, J.L., 2002, *Classical Mechanics*, 3rd ed., Addison-Wesley. Good introductory section 3.12 describing some exact solutions and some aspects of the restricted three-body problem, but with one major error and other minor problems.

Hestenes, D., 1987 and 1999, *New Foundations for Classical Mechanics*, 1st and 2nd ed., D. Reidel. LSU's library has the corrected 1st edition. The overall flavor of this book is fairly mathematical and should be considered more as an introduction to geometric algebra and spinors. However, section 5 of chapter 6 derives correctly the results described in Goldstein and can be read profitably without familiarity with the rest of the machinery.

Montgomery, R., 2001, *A New Solution to the Three-Body Problem*, Not. Am. Math. Soc. **48**, 471-481. Contains some curiosities, URLs to animations, and the references to the classical work of Euler (in Latin) and Lagrange (in French).

Szebehely, V.G., 1967, *Theory of Orbits*, Academic Press. The most comprehensive treatment of the restricted three-body problem in the literature. Contains vastly more than you ever want to know unless you plan to become an expert in calculating space probe orbits or do research in certain areas of stellar dynamics.

Szebehely, V.G. & Mark, H., 1998, *Adventures in Celestial Mechanics*, 2nd ed., Wiley. A very readable introductory text on orbital dynamics with historical digressions and an account of modern results on chaos, strange attractors, and orbital stability.

Valtonen, M. & Karttunen, H., 2006, *The Three-Body Problem*, Cambridge University Press. This book was just published and, based on what I've been able to glean from the web, it looks destined to become a must read for theoretical astrophysicists working on widely diverse fields like solar system dynamics, globular clusters, and active galactic nuclei. Mauri Valtonen is the best known theorist still pursuing the slingshot mechanism for quasars.